INFLUENCES OF AIR, NITROGEN, AND OXYGEN ON THE PHOTOCONDUCTIVITY OF ORGANIC TRIMETHYL PHENYL DIAMINE THIN FILM

Nazrul Anuar Nayan
Dept. of Electric, Electronic and System Engineering
Faculty of Engineering and Built Environment
Universiti Kebangsaan Malaysia
UKM Bangi, Malaysia
Email: nazrul@ukm.edu.my

Khairul Anuar A. Rahman
Dept. of Electronics and Computer Technology
Faculty of Engineering Technology
Universiti Teknikal Malaysia Melaka, Malaysia
Email: khairulanuar@utem.edu.my

ABSTRACT

Organic materials were previously used as insulators in electrical technology. These materials, however, are currently used as conductors once their photoconductivity was confirmed and studied. Attention is focused on the practical use of organic electroluminescence devices, such as light-emitting diodes. Moreover, the applications of organic transistors have received increased research attention due to their advantages, including lower manufacturing cost. These active materials are processed at low temperatures from a wide range of bendable materials, such as plastic or paper, which meet the requirements for miniaturization and integration. Nevertheless, the low mobility of electrons in solid state remains problematic. The preparation method of thin films confers a structure that resembles that of amorphous semiconductor substances to organic semiconductors. Therefore, this study investigated the influence of air on the photoconductivity, photoconductivity degradation, and residual decay of trimethyl phenyl diamine thin films. Experiments in vacuum, nitrogen, and oxygen conditions were also performed.

Keywords: Photoconductivity, semiconductor, TPD, residual decay

INTRODUCTION

The weak conductivity of organic compounds, which were previously considered as nonconductive, was first discovered in 1948. In 1954, Hiroo Inokuchi and Hideo Akamatsu conducted ground-breaking studies that systematically investigated the intermolecular electrical conductivity of violanthrone, an organic molecule that consists of nine benzene rings. Violanthrone acts like a semiconductor in a manner that is similar to that of inorganic materials (Hiroo, 2007). This finding is a stepping stone for the development of organic semiconductor applications, such as displays, photovoltaics, and electronic components. Organic field-effect transistors and organic light-emitting diodes remain as the fundamental electronic building blocks of organic electronic circuits (Mohan, 2014). Therefore, small electronic components are the basis for the development of electronic devices.

Compared with inorganic semiconductors, organic semiconductors are more easily tailored for specific applications (Stephen, 2004). For example, compounds that contain conjugate bonds, such as –C=C–C=, have large optical nonlinearities and thus have potential applications in optoelectronics. In addition, organic semiconductors have low cost, mechanical flexibility, synthetic versatility, solution-processability, and high-purity; these materials can be tailored into high-performance photoconductive thin films (Day *et al.*, 2008 and Rosalba, 2013). Molecular design for a variety of molecular structures is easily performed by combining atoms with different internal and intermolecular forces. Chemical formulas are changed to suit a specific application. The bandgaps of organic semiconductors are easier to change than those of inorganic semiconductors. Trimethyl phenyl diamine (TPD) is widely used as a material for typical photoconductive organic films given its simple structure and fundamental photoconductivity (Sato *et al.*, 2008). Therefore, the photoconductivity of TPD films has been extensively studied. The steady-state photoconductivity of other organic semiconductors has also been investigated (Irkhin *et al.*, 2015). Over time, the photoconductivity of organic semiconductor films tends to increase in air and tends to decrease in a vacuum condition (Shimakawa *et al.*, 2007). These studies have revealed that photoconductivity degradation and residual decay occur during irradiation.

TPD (Figure 1) has two sets of triphenyl amine with an ionization potential of approximately 5.4 eV. TPD also possesses an aromatic amine compound with ~10^{-3} cm^2/Vs positive hole mobility. Holes are the dominant carrier in TPD films. TPD is a representative charge transport material given its relatively high mobility, which can be increased by one digit via doping. The use of TPD as a hole transport layer in organic electroluminescence has been recently studied (Rudati *et al.*, 2015). Furthermore, the hopping photoconductivity and reasonable physical parameters of TPD have been found to consist of hopping relaxation time, recombination time, and diffusion coefficient of charge carriers (Shimakawa *et al.*, 2007). These characteristics contribute to the photoconductivity of TPD.

Figure 1: Chemical structure of TPD
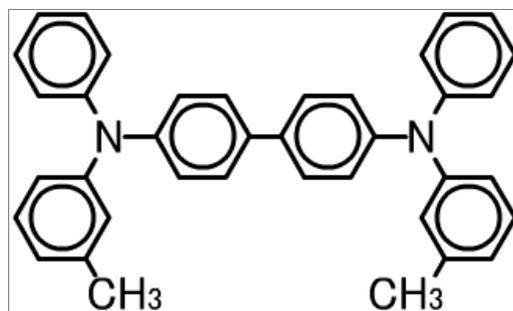
Similar to a general semiconductor, the band theory can be applied when an electron or a positive hole becomes the carrier in an organic polymeric semiconductor. However, unlike in crystal semiconductors, various localized levels can form in organic polymeric conductors because of its irregular structure. Therefore, organic conductors resemble an amorphous semiconductor with an extremely rugged conduction and valence band, as well as a band gap value that remains constant. Given that various state densities exist at the local level, the band edge does not remain sharp but rather resembles the band gap of a crystalline semiconductor (band tail). The band edge is determined by the energy used with sharp mobility change given the low mobility of the captured carrier at the localized level. In this study, the influences of air, oxygen, and nitrogen on the photoconductivity of TPD film were investigated.

METHODS

Prior to TPD film preparation, the glass substrate (Corning 7059) was ultrasonically cleaned at 10, 50, and 100 Hz in both acetone and ethanol at 20 cycles per solvent. Then, a vacuum evaporation system (Ulvac Corp. K.K EBH-6 type) was used to deposit a 0.5-µm thick TPD thin film onto the glass substrates via the thermal evaporation technique. Deposition was conducted in a vacuum condition of approximately 2×10^{-6} Torr at room temperature. The Au electrode was deposited in a vacuum deposition (resistive heating) with a mask.

Figure 2 shows the main equipment used in this study. The apparatus consisted of a cryostat, He–Cd laser, measurement display, and plotting software. The cryostat was an air-tight enclosure in which the samples were placed during measurement. The sample used was a gap-type cell. First, Ag powder paste was used to mount the gold wire on the electrodes of the sample. The sample was then pasted on the wall of the cryostat. Next, the gold wire was connected with an external measuring terminal and wiring for the DC power source. After the sample was installed, the cryostat was vacuumed with the rotary pump. The sample and photoconductive material (TPD thin film) were irradiated with the He–Cd laser (λ = 325nm). Neutral density filter sets were used to obtain the desired density. The laser entered through a point in the glass windows. A three-way valve was connected to the cryostat to switch between the rotary pump-cryostat and the gas canister-cryostat. Oxygen and nitrogen gases were then injected.

A temperature controller and frozen compressor were not used because the experiments were conducted at room temperature. The internal temperature of the cryostat was measured using a thermocouple. Labview was used for accurate and long-time data plotting. In this study, the majority of the data were obtained after 96 h. The changes in the photocurrent were easier to observe when the laser was alternately turned off or on. The shortest measurement speed was set to 0.5 s.

Figure 2: Diagram of measurement method
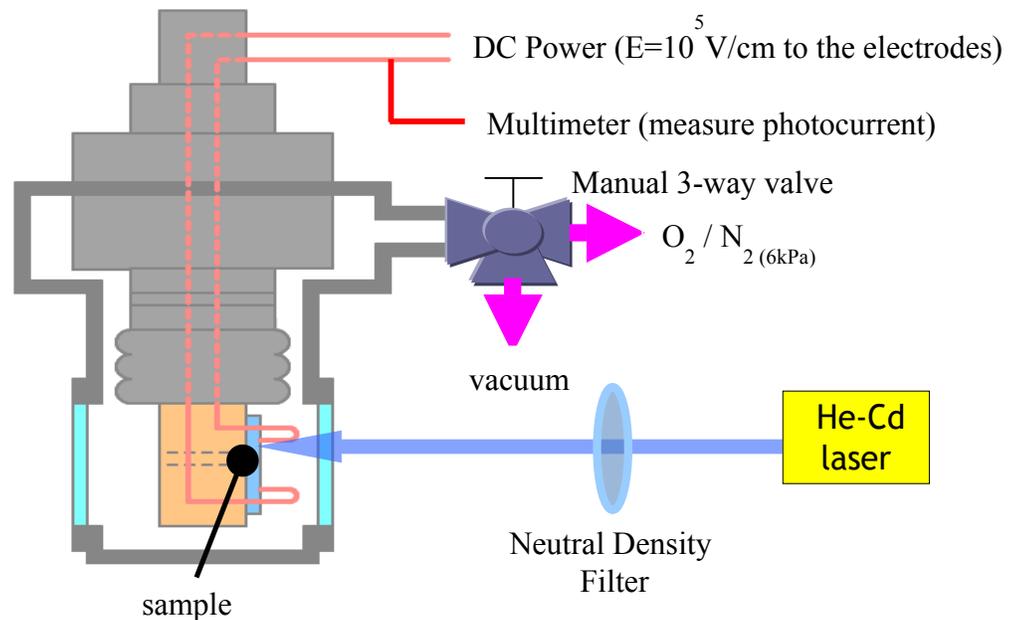
An electric field of 10^5 V/cm was applied to the electrodes of the sample. The sample was irradiated with a single power of 72 mW/cm^2 He–Cd laser at 3.82 eV. Photocarriers were induced by irradiation. The estimated charge carrier generation rate was 7.2×10^{21} cm^{-3} s^{-1}. The photocurrent in TPD, which was set in the cryostat, was measured in vacuum, air, O$_2$, and N$_2$ conditions. All experiments were performed at 300 K. Experimental data were fitted to stretch exponential functions.

For the photon frequency, v was calculated as 9.23×10^{14} s^{-1} (hv = 3.82eV) at 1 mW/cm^2. The number of photons deduced from the laser power was divided by hv and is

$$N_0 = 0.001[W\,cm^{-2}] / (9.23 \times 10^{14}[s^{-1}] \cdot 6.63 \times 10^{-34}[Js]) = 1.63 \times 10^{15}[cm^{-2}s^{-1}].$$

Given that the reflection R is 30%, the thickness of sample is 0.5 μm and the absorption coefficient $\alpha = 10^5$ cm^{-1}, the photogeneration rate was calculated as follows:

$$G = N_0(1 - R) \cdot \alpha = 1.63 \times 10^{18} \cdot 0.7 \cdot 10^5 = 1.14 \times 10^{20}[cm^{-3}s^{-1}].$$

The increase in the current after the laser irradiation ($f_1(t)$) and the attenuation of the current after the laser is intercepted ($f_2(t)$) were studied by fitting the graph with the stretch functions:

$$f_1(t) = A\,(1 - \exp\,[-\,(t/T)^\beta])$$

And

$$f_2(t) = A\,\exp\,[-\,(t/T)^\beta]$$

, respectively. Here, $_T$ [sec] is the effective response time to show the response speed and β is the dispersion parameter. For example, in $f_1(t)$, $_T$ = 100 s and β = 0.26, whereas in $f_2(t)$, $_T$ = 1.24 s and β = 0.47. In $f_1(t)$, the value of $_T$ is the time until saturation. This value depends on the laser power. A higher power indicates a smaller $_T$ value.

RESULT AND DISCUSSION

As shown in Figure 3, the photocurrent increases when air is injected into the cryostat in vacuum condition at t = 30 min. In air, the photocurrent in TPD is 5 nA to 8 nA compared with that in vacuum, which is approximately 2.5 nA. The photocurrent returns to its original value when the TPD is returned to the vacuum condition. The photocurrent increases again after the air is replaced by vacuum in the next cycle at t = 300 min. Given that this behavior is reversible, it is a physical rather than a chemical reaction.

Figure 3: Photoconductivity in vacuum and air conditions during light irradiation
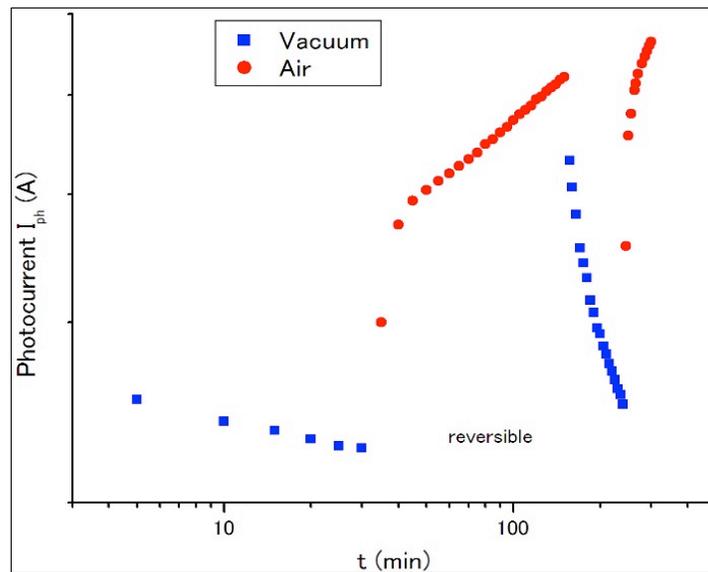
Air is composed of 78% molecular N_2, 20% O_2, 1.9% Ar, and small amounts of Ne, He, CH_4, Kr, H, N_2O, and Xe. Air contains variable concentrations of water vapor (H_2O), ozone (O_3), CO_2, and SO_2. O_2 is the most active gas for chemical or physical reactions.

The photoconductivity of TPD in vacuum is measured before introducing air and gas. For this experiment, the photocurrent measurements are performed when the laser is turned on and off. The changes in the photocurrent of the samples are observed in the dark, after irradiation, and after laser interception. Table 1 shows the processing times when the laser is on and off. The first light is on after 5 min, and the final interception or light off is after 97 h.

Table 1: Laser On/Off time

method	
Time [hh:mm:ss]	Laser On/Off
00:05:00	ON
02:00:00	OFF
02:01:00	ON
04:00:00	OFF
04:30:00	ON
05:30:00	OFF
72:00:00	ON
77:00:00	OFF
96:00:00	ON
97:00:00	OFF

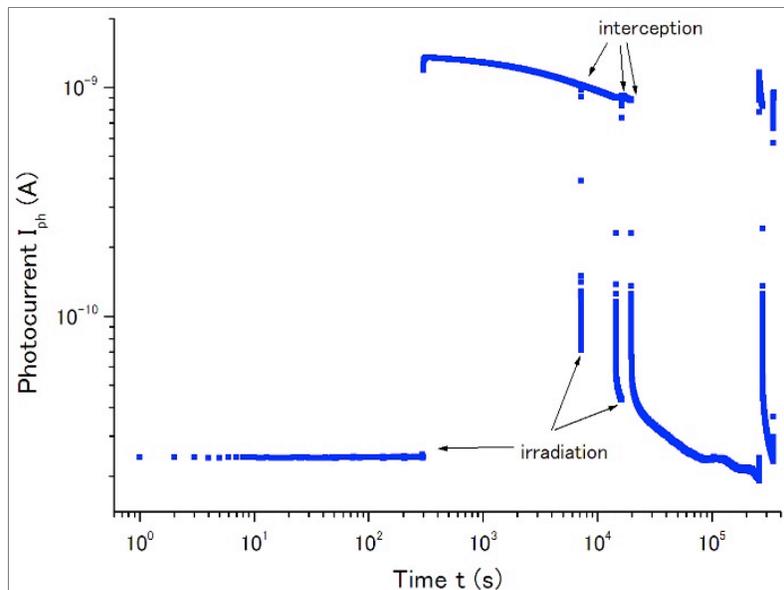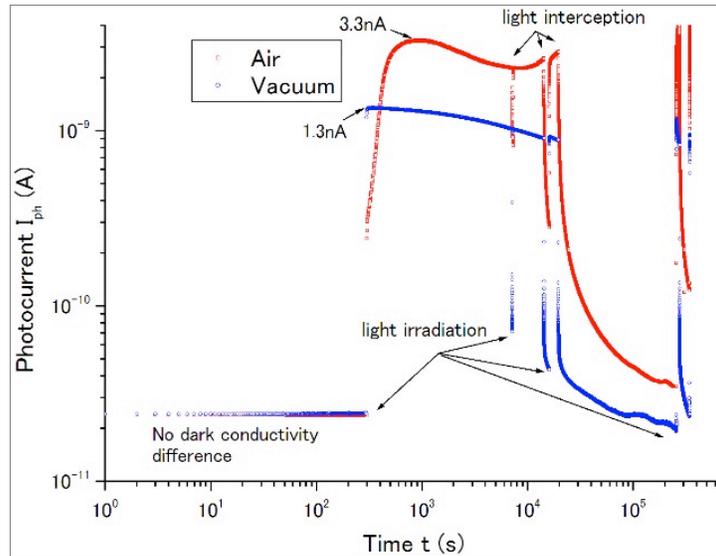**Figure 4: Photocurrent in vacuum conditions**

Figure 4 shows the photocurrent of TPD films in vacuum conditions. The dark current is approximately 25 pA. Irradiation begins at 300 s. The photocurrent increases to a peak of 1.5 nA. Photoconductivity degradation occurs after the photocurrent reaches the maximum value. Residual decay is observed after the light is turned off. As a reference, the photocurrent in a vacuum is measured with the light on/off as mentioned in Table 1. The values are shown as irradiation (laser on) and interception (laser off).

Figure 5: Photoconductivity in vacuum and air conditions

A separate experiment is conducted in air atmospheric condition. Then, the results for air and vacuum conditions are compared. Figure 5 shows the photocurrents under the air and vacuum conditions. No significant difference is observed before irradiation (dark). The maximum value of photocurrent in air is 1.5 times more than that in vacuum. After the first interception (t = 2 h), the photocurrent increases in the air condition, which is different from that in the vacuum.

To further study the effect of air on the photoconductivity of TPD, O_2 gas and N_2 gas were added at 6 kPa. First, the cryostat was vacuumed. Then using the manual-3-way valve, the direction was changed from the vacuum compressor to the gas canister. A fresh sample of TPD was used per experiment under the vacuum, air, O_2, and N_2 conditions to clearly differentiate the effect of each condition on the sample.

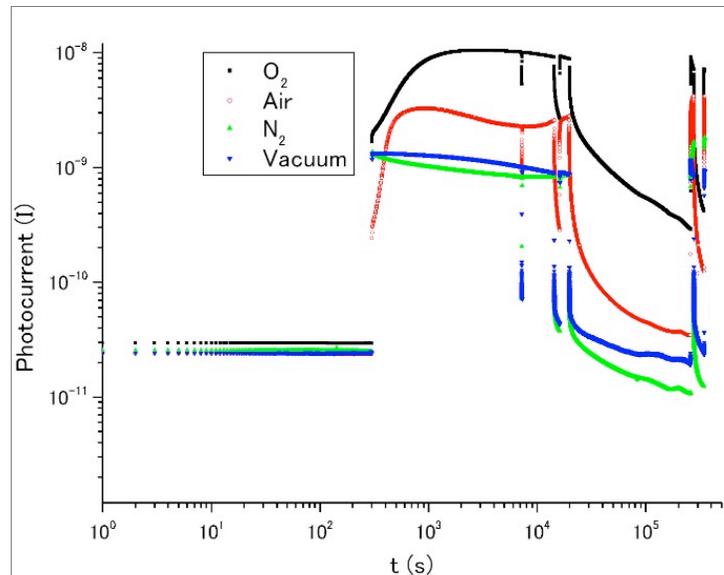**Figure 6: Photoconductivity in air, O_2 and N_2 conditions**

Figure 6 shows that a dark current of 20 pA to 30 pA, the photocurrent is not significantly different for all four conditions. After irradiation, the photoconductivity is higher in O_2 condition, followed by that in air, in vacuum, and lastly in N_2. In O_2, the maximum photocurrent is 10.5 nA, whereas the maximum value in N_2 is only 1.5 nA. Photoconductivity degradation occurs in all conditions; however, the highest speed to degradation is observed in N_2, followed by air and O_2. An upward trend of photocurrent is observed in air condition after the 1st laser interception (t = 2 h). Degradation trends continue in O_2 and N_2. When irradiation starts after 66 h, an upward trend in photoconductivity is observed in N_2 and air. The physical phenomenon for this finding is still unknown. Light-induced photoconductivity degradation occurs in all conditions.

N_2 gas is an inactive gas that is widely used in the semiconductor industry. The amount of water vapor in N_2 used in this study is 10 parts per million (ppm). The N_2 gas used in this study contained only $\sim 1 \times 10^{13}$ water vapor molecules. In this study, 6 kPa N_2 is used. Hence, the effect is actually smaller. The number of carriers is 10^{16}. This value is still high compared with 10^{13}, which is the same as the number of the water vapor molecules. Therefore, the effect of water vapor is insignificant in this study.

Another experiment is conducted to confirm the effect of O_2 on photoconductivity. The objective is to determine the difference in photoconductivity when light is initially irradiated in vacuum condition and after O_2 injection. As shown in Fig. 7, photoconductivity increases to approximately 8 nA. No difference is observed in the graph compared with O_2 in Fig. 7. This result confirms that the value of the photocurrent of the TPD under O_2 condition is the same even when O_2 is injected after the first irradiation.

Figure 7: Photocurrent changes when irradiation starts in vacuum condition then to O_2
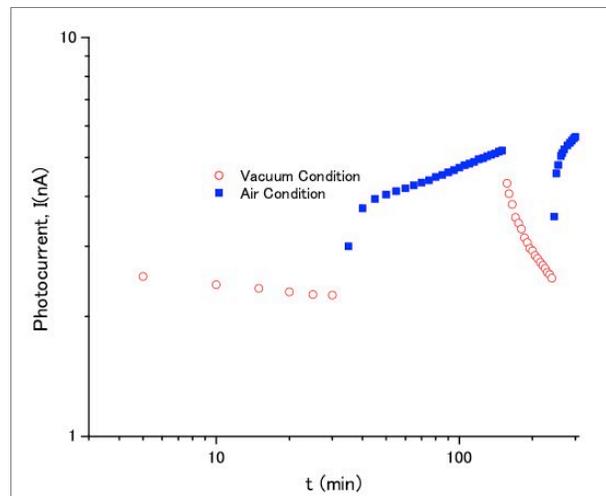
Photoconductivity degradation is further studied because light-induced photoconductivity is a crucial characteristic of semiconductor materials. Photoconductivity decreases when light is continuously irradiated to the semiconducting photoconductive materials. Therefore, in the semiconductor industry, materials are only used after degradation is completed. However, the steady-state degradation of photoconductivity is poorly understood. Therefore, the time required for the material to recover to its original initial value after the light is cut off should be determined.

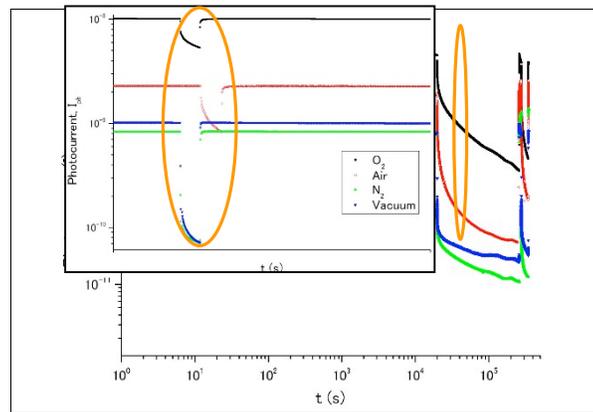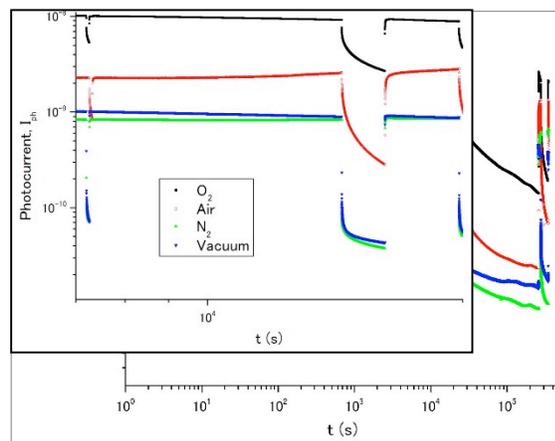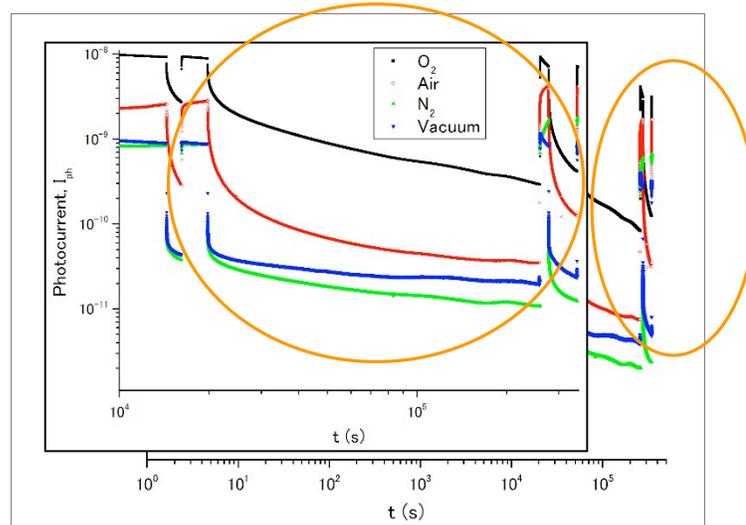**Figure 8: Photoconductivity degradation after 60 s light interception**

Figure 8 shows that in almost all conditions, degradation does not recover when the laser is cut for 60 s after irradiation for 1 h and 55 min.

Figure 9: Photoconductivity degradation after 66 hours light interception

In Figure 9, the light is cut off for 30 min after 3 h and 54 min of irradiation. Photoconductivity continues to exhibit a similar degradation pattern. Therefore, the recovery of photoconductivity to its original value in TPD requires longer than 30 min.

Proceeding – Putrajaya International Built Environment, Technology and Engineering Conference (PIBEC2017), 27 – 28 March, 2017. Hotel Bangi-Putrajaya,Bangi, Malaysia.

ISBN: 978-967-2072-04- 1

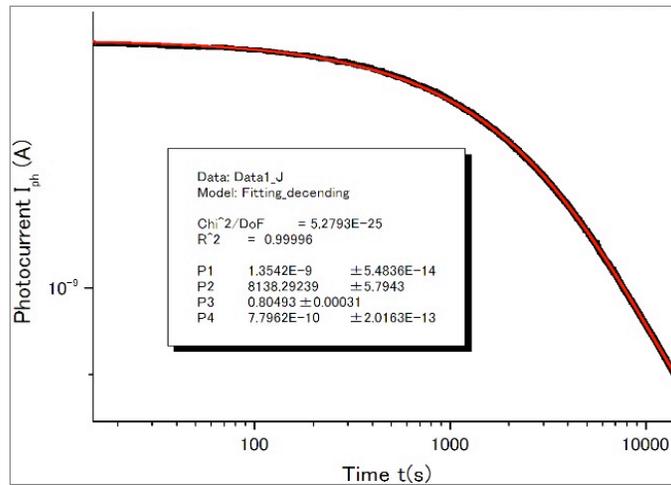**Figure 10: : Photoconductivity degradation after 66 hours light interception**

To further investigate the permanence of photoconductivity degradation, the light is again cut off for 66 h after 4 hr and 54 min of irradiation. Figure 10 shows that most of the conditions recover when the photocurrent is higher compared with that exactly before the cut-off. The photocurrent shows an upward trend in N_2. Another degradation trend is observed in O_2 and vacuum conditions. The upward trend of the photocurrent is also observed in air because 78% of the air is N_2. The reason for this upward trend in N_2 is unknown.

A graph is plotted to show the degradation phenomenon in all conditions. The data from the maximum photocurrent point until the cut off are fitted to a stretch function. Only the attenuation effective response time $_T$ and the dispersion parameter β are measured in this experiment. The results from those fittings are shown in Table 2.

Table 2: $_T$ and β value for photoconductivity degradation

$f_2(t) = A \exp [- (t/T)^{\beta}]$		
Condition	T [s]	β
Vacuum	8138	0.80
Air	2039	1.28
O_2	12476	1.49
N_2	724	0.47

Figure 11: Fittings by origin lab

The τ and beta for both photoconductivity degradation and decay are obtained by fitting the graph with the stretched exponential function.

Residual decay is the remaining photocurrent after the light is intercepted. The fitting with stretched exponential function of the equation is used again to measure attenuation response time and dispersion time. The results from the fitting are shown in Table 3.

Table 3: τ and β value for residual decay in TBD

$f_2(t) = A \exp\left[-(t/T)^\beta\right]$		
Condition	T [s]	β
Vacuum	0.07	0.10
Air	147	0.29
O_2	2139	0.39
N_2	478	0.22

Table 4 shows the measured time to the ½ value of the photocurrent in all conditions. The longest time is observed in O_2 condition at 291 s, followed by in air at 32 s, and in N_2 at 1 s.

Table 4: Data showing the decay time to the half (1/2) value

Decay Time	
Substances	½ value decay time [s]
O_2	291
Air	32
Vacuum	1
N_2	1

The increase in photoconductivity in air is reversible, indicating that this response is a physical reaction. Considering that oxygen attracts electrons, the number of photo-created electrons decreases with oxygen content and increases the lifetime of holes, which are the dominant carriers in TPD films.

CONCLUSION

This paper present photoconductivity measurement of TPD under vacuum, air, nitrogen and oxygen conditions. First, air produces about 1.5 times higher photocurrent compare to in vacuum condition. Second, conductivity in dark shows

no difference in all conditions. Third, light induced photoconductivity occurs in all conditions. Then, O_2 increases the photoconductivity and give a larger $_T$ in both degradation and residual decay. Besides, degradation occurs in all conditions and its recovery takes more than 65 hours.

REFERENCES

Day, J., Subramaniam, S. Anthony, J. E., Lu, Z., Twieg, R. J. & Ostroverkhova, O. (2008). Photoconductivity in organic thin films: from picoseconds to seconds after excitation. *Journal of Applied Physics*, 103.

Hiroo, I. (2007). Laureate Lectures, *New Developments in Organic Semiconductor and Conductors*, Kyoto Prize Workshop in Advanced Technology.

Irkhin, P., Najavoc, H & Podzorov, V. (2015). Steady-state photoconductivity and multiparticle interactions in high-mobility organic semiconductors, *Sci Rep.*, 5.

Mohan, V. J. (2014). Organic semiconductors: past, present and future. *Electronics*, 3, 594-597.

Rosalba, L. (2013). A study on defects in organic semiconductors for field effect transistors. Thesis of Doctorate.

Rudati, P. S., Mueller, D. C. & Meerholz, K. (2015). The I-V characteristics of organic hole-only devices based on crosslinked hole-transport layer. *Journal of Applied Research and Technology*, 13(1), 253-260.

Sato, T., Yonezawa, K., Shimakawa, K & Naito, H. (2008). Photoconductivity in organic TPD film: effect of photoadsorption of O_2 and N_2. *Journal of Non-Cystalline Solids*, 2866-2869.

Shimakawa, K., Nazrul Anuar, Yonezawa, K & Sato, T. (2007). Dynamics of photoconductivity in organic TPD films. Journal of Optoelectronics and Advanced Materials, 9(1), 65-69.

Stephen, R. F. (2004). The path to ubiquitous and low-cost organic electronic appliances on plastic. *Nature*, 428, 911-918.